The presence of the slit in the body of the segment somehow perturbs the flow; however, the perturbations on the shock front damp out approximately 10-fold within the distances $\sim 3\lambda$ (λ is the perturbation wavelength) [3]. In our case λ is on the order of the slit width. The minimum distance within which a velocity jump occurs in the experiments described (for $h/R = 0.9$) is $x_1 = 12$ mm, which is much greater than the slit width of ~ 1 mm. The presence of the slit, if it does exert an influence, will exert an influence which is more often toward the diminution in the effect of cumulation.

In conclusion, let us note that more special forms of the hollow in the end face of the plug at the end of the shock-tube channel can result in a still greater effect. In particular, the shape of a segment surface in which collapse of the transverse wave would be realized in the form of a cylinder or of a cone with apex turned toward the bottom of the segment can result in magnification of the effect.

LITERATURE CITED

1. E. E. Meshkov, "Reflection of a plane shock from a rigid concave wall," Izv. Akad. Nauk SSSR, Mekh. Zhidk. Gaza, No. 4, 33 (1970).
2. H. Schardin, "Ein Beispiel zur Verwendung des Stosswellenrohres für Probleme der instationären Gasdynamik," Z. Angew. Math. Phys., 9, Nos. 5/6, 606-621 (1958).
3. A. A. Kovitz and M. G. Briscoe, "Stability of a plane shock wave in free space and in the presence of rigid or interfacial boundaries," J. Acoust. Soc. Amer., 45, No. 5, 1157-1165 (1969).

STREAM MODELS APPROXIMATING THE PROPERTIES OF SUPERSONIC JET FLOWS

V. G. Dulov

UDC 533.6.011:51.72

§1. A free supersonic off-design jet is often the incoming stream or background for more complex phenomena and processes (Fig. 1, where the dashes are contact discontinuities and the solid lines are shocks). Hence, the simplicity of the analytical description of such jets is an important condition for the successful solution of problems of a higher degree of difficulty than the jet itself. Let us examine the following most simple model of a free jet: a one-dimensional supersonic stream moves in a channel with permeable walls. The escape velocity through the holes in the walls equals the local speed of sound. By increasing the area of the holes, we obtain a one-dimensional stream in the limit in which the velocity along the normal to the cylindrical surface equals the speed of sound. If the escape occurs into a medium with counterpressure, then a shock will appear at some intermediate secton of the channel. Its position is easily determined and corresponds practically exactly with the position of a central shock in an underexpanded jet. A simple improvement of this rough model permits obtaining good qualitative results relative to all the fundamental supersonic jet parameters in the free expansion domain (domain I in Fig. 1). The flow in a channel with variable cross-sectional area and with permeable walls is considered as the approximating stream. In the limit, the role of the permeable wall is played by one of the characteristic surfaces, which converge with the nozzle edge whose shape is determined to fourth-order accuracy relative to the angle of stream divergence.

Let us form the mathematically presented considerations by using the following notation: x, y are the coordinates in the plane of the axial stream section; u, v are velocity projections on the x, y axes; w is the absolute value of the velocity; ϑ is the slope of the velocity vector to the axis of symmetry; M is the Mach number; α is the Mach angle ($\sin \alpha = 1/M$); k is the ratio of the specific heats; p is the pressure; ρ is the density; h is the static heat content; h_m is the total heat content; S is the entropy; ψ is the stream function; and the equation of state is assumed given in the form h(p, S). The parameters on the jet boundary are denoted by the subscript H and on the nozzle exit by a. We consider all the quantities dimensionless: the coordinates are

Krasnoyarsk. Translated from Zhurnal Prikladnoi Mekhaniki i Tekhnicheskoi Fiziki, No. 4, pp. 37-60, July-August, 1976. Original article submitted December 26, 1975.

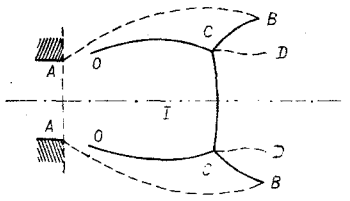

Fig. 1

referred to the radius of the nozzle exit section, the velocities to the magnitude of the maximum stationary escape into a vacuum $w_m = \sqrt{2h_m}$, and the pressure to the stagnation pressure in the initial isentropic flow. Under such conditions the Bernoulli equation is written as $w^2 + h = 1$.

Let us perform the standard passage to the plane of the hodograph variables (u, v) in the equations of motion. For problems with axial symmetry such an approach is ordinarily useless for investigations of exact formulations and methods, but can turn out to be quite convenient for the construction of approximate solutions. Let us go over to the variables ξ, η instead of u, v in equations written in the hodograph plane, by using the relationships

$$\xi = w^2 = 1 - h = u^2 + v^2; \quad \eta = v^2 = (1 - h)\sin^2\vartheta.$$

It follows from the Euler equation transformed to the variables mentioned that a characteristic flow function $\varphi(\xi, \eta)$ exists such that

$$\varphi_\xi = y^2/2h_p - \psi/2\sqrt{\xi - \eta}; \quad \varphi_\eta = \psi/2\sqrt{\xi - \eta}.$$

The Euler equation is satisfied identically for any function φ. By using the continuity equation, expressions are obtained for derivatives of the axial coordinate x with respect to the variables ξ, η:

$$x_\xi = \sqrt{h_p}\,\frac{(\xi - \eta)\,[\varphi_{\xi\xi} + j(\varphi_\xi + \varphi_\eta)]}{2\sqrt{2\eta\,(\xi - \eta)\,(\varphi_\xi + \varphi_\eta)}}; \quad x_\eta = \sqrt{h_p}\,\frac{\varphi_\eta + 2(\xi - \eta)\,\varphi_{\xi\eta}}{2\sqrt{2\eta\,(\xi - \eta)\,(\varphi_\xi + \varphi_\eta)}}, \tag{1.1}$$

where $j = -h_{pp}/h_p^2$. Eliminating x from (1.1) by cross differentiation, we obtain a second-order partial differential equation of Monge–Ampere type with the quasilinear part

$$2(\xi - \eta)\,\eta\,(\varphi_{\xi\eta}^2 - \varphi_{\xi\xi}\varphi_{\eta\eta}) - \eta\{2[1 - (\xi - \eta)\,j](\varphi_\xi + \varphi_\eta) - \varphi_\eta\}\varphi_{\eta\eta} -$$
$$- 2\eta(2\varphi_\xi + \varphi_\eta)\,\varphi_{\xi\eta} - [(2\xi - \eta)\,\varphi_\eta + 2\xi\varphi_\xi]\,\varphi_{\xi\xi} - 2\xi j(\varphi_\xi + \varphi_\eta)^2 - (1 - \eta j)\;\varphi_\eta(\varphi_\xi + \varphi_\eta) = 0. \tag{1.2}$$

This equation is homogeneous in the desired function and all its members contain derivatives in the form of products of two partial derivatives, where the coefficients of these products are polynomials of not higher than the second degree in η. Such a structure of the equation permits seeking the solution as a power series in the variable η. It should be expected that such an expansion is effective when the flow has primarily an axial direction. Let us introduce the constant parameter ε which characterizes the order of the angle ϑ in the motion domain under consideration, and let us consider ε a small quantity. Evidently $\eta \sim \varepsilon^2$. Hence, we introduce the deformed variable $\bar{\eta}$ from the relationship $\eta = \varepsilon^2\bar{\eta}$ and we seek the solution in the form of the expansion

$$\varphi = \sum_{k=0}^{\infty} \varepsilon^{2k}\varphi_k(\xi, \bar{\eta}).$$

Equating the expression for identical powers of ε in (1.2) to zero, we obtain recursion relations for the coefficients φ_k. Since ε takes no part in the subsequent considerations, let us set $\varepsilon = 1$, i.e., we return to the undeformed variable η:

$$(2\xi j - 1)(\varphi_{k\eta\eta} - (1/\eta)\varphi_{k\eta}) = F_{k-1}; \quad F_{-1} = 0 \;(k = 0, 1, 2\ldots).$$

In the general case F_{k-1} can be expressed for $k > 0$ in terms of the function φ_n with smaller subscripts ($n < k$). Let us consider $2\xi j \neq 1$, i.e., $M \neq 1$. Then we find

$$\varphi_0 = C\eta^2/2 + D,$$

where C and D are arbitrary functions for the variable ξ

$$\varphi_1 = [1/(2\xi j - 1)]\ \{[4\xi(CC'' - C'^2) + (5 + 2\xi j)CC' + 3jC^2]\eta^3/3 + [(1 + 2\xi j)D' + 4D'']\eta\}.$$

Here the primes denote derivatives with respect to ξ. In the approximation $\varphi = \varphi_0 + \varepsilon^2\varphi_1$, the flow is described by the formulas

$$\begin{aligned} x &= \int \left(\sqrt{h_p/8\xi}\right)(2\xi j - 1)\,C d\xi + \left(\sqrt{h_p/8\xi}\right)(C + 4\xi C')\,\eta; \\ y^2/2 &= h_p C^2\,\eta + [h_p(2\xi j - 1)]\{[4\xi(CC'' - C'^2) + 4(1 + \xi j)CC' + \\ &\quad + 3jC^2]\eta^2 + 2(D' + 2\xi D'')\}. \end{aligned} \tag{1.3}$$

Evidently, $D \equiv 0$ if the flow contains the axis of symmetry. By using the solution in the form (1.3), we give a mathematical description of the two above-mentioned free jet models.

One-Dimensional Model. It can be seen that the first members in the right sides of (1.3) agree exactly with the formulas of the one-dimensional theory of stationary flows in channels with variable cross-sectional area. Only the arbitrary function $C(\xi)$, related to the channel shape, is not usually introduced. For the purposes of the problem under consideration, such a description is more convenient. Thus, let

$$x = \int \left(\sqrt{h_p/8\xi}\right)(2\xi j - 1)\,C d\xi; \quad y^2/2 = h_p C^2 \eta. \tag{1.4}$$

The boundary conditions in the one-dimensional model are $\vartheta = \alpha$ on the characteristic surface $y = 1$ (α is the Mach angle), i.e., $\eta = (1-\xi)/M^2$, and, therefore, $C^2 = M^2/2h_p(1-\xi)$. For an ideal gas with constant specific heats $M^2 = [2/(k-1)]\xi/(1-\xi)$. Substituting C in the first of formulas (1.4) and integrating, we obtain

$$x = M/(k-1) - [(k+1)/(k-1)^2]\ \sqrt{(k-1)/2}\operatorname{arctg}(M\sqrt{(k-1)/2}) + \text{const}. \tag{1.5}$$

This formula can be used to describe the Mach number distribution along the jet axis although it yields an asymptotically false result as $M \to \infty$.

The shock in the simulating channel is set at that section where the critical pressure p_1 becomes equal to the pressure in the surrounding medium p_H for escape into a medium with counterpressure, and if it is assumed that the pressures in the provisional holes and in the channel are equalized, then the pressure p_2 behind the shock must be set equal to the pressure in the surrounding medium. If (1.5) is used, then the second assumption yields a better agreement with experimental results, but if the exact law for the Mach number distribution along the jet axis is used (for instance, as obtained by the method of characteristics), then the first assumption results in more exact values of the central shock coordinate x_s. Hence, the x_s are obtained somewhat less true. Under the condition $p_2 = p_H$, the x_s turn out to be greater than the experimental for exact M(x). The most exact values of x_s are obtained if the approximate formula (1.5) is used with the condition $p_1 = p_H$. Mutual cancellation of the errors apparently occurs here. For gases with constant specific heats, we obtain an equation for the Mach number M directly in front of the shock front from the adiabatic condition and the formula for the pressure behind a normal shock

$$\frac{p_i}{p_a} = \left(\frac{2k}{k+1}M^2 - \frac{k-1}{k+1}\right)\left(\frac{1 + \frac{k-1}{2}M_a^2}{1 + \frac{k-1}{2}M^2}\right)^{k/(k-1)}, \quad i = 1 \text{ or } 2.$$

The shock coordinate x_s is determined by means of the M found.

Second-Approximation Model. Let us use the complete formulas (1.3) to describe this model. The imaginary permeable surface bounding the channel is a characteristic. The normal velocity component along it equals the local speed of sound. Let us use the equation of the characteristics in the form

$$\begin{aligned} dy/dx &= \operatorname{tg}(\vartheta - \alpha); \\ d\vartheta - \frac{\cos^2\alpha}{(k-1)/2 + \sin^2\alpha}\,d\alpha - \frac{\sin\alpha\cdot\sin\vartheta}{\cos(\vartheta-\alpha)}\,\frac{dx}{y} &= 0. \end{aligned} \tag{1.6}$$

Since $\alpha \sim \vartheta$, then $h \sim \vartheta^2$ and, therefore, h is a small quantity whose squares can be neglected, i.e., in such a formulation we deal with the hypersonic approximation. Substituting x, y in the form of (1.3) and retaining the first two members of the expansion in h, we obtain the solution in parametric form after tedious computations:

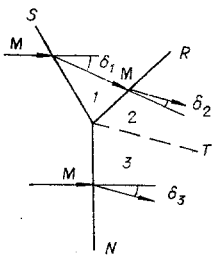

Fig. 2

$$x = x_0(h) - \frac{1}{4}\left(\frac{h_0}{h}\right)^{\frac{\gamma}{2}} \frac{M_0}{\sqrt{1-h_0}} \frac{4\beta(1-h)-1}{\sqrt{1-h}\, e^{\beta(h_0-h)}}\eta;$$

$$x_0(h) = \frac{M_0 e^{-\beta h_0}}{\sqrt{1-h_0}}\left[\left(\frac{h_0}{h}\right)^{\frac{\gamma}{2}}\left(1 - \frac{\beta - \frac{k}{2}}{\frac{2}{\gamma}-1}h\right) - \left(1 - \frac{\beta-\frac{k}{2}}{\frac{2}{\gamma}-1}h_0\right)\right]; \qquad (1.7)$$

$$y = \left(\frac{h_0}{h}\right)^{\frac{\gamma}{2}} \frac{M_0}{\sqrt{1-h_0}} \frac{1-\left(\beta-\frac{3}{4}\right)}{e^{\beta(h_0-h)}}\sqrt{\eta},$$

where $\gamma = 1/(k-1)$; the subscript 0 denotes the initial parameters for the characteristic converging to the nozzle edge; the parameter β remains undetermined in the problem formulation under consideration and can be used to satisfy an additional requirement. Formulas (1.7) describe the parameter field in the domain of free jet expansion and are in good agreement with computations by the method of characteristics for a suitable selection of β. The second of the formulas yields the distribution of h (or the Mach numbers) along the jet axis. In contrast to (1.5) it has the correct asymptotic as $h \to 0$ ($M \to \infty$).

§2. Stream models simulating the flow in the free jet-expansion domain, independent of counterpressure and the presence of an obstacle, were examined above. The flow in all the remaining sections of the jet is essentially determined by the counterpressure and, in the case of restricted escape into domains adjoining an obstacle, also by the position and shape of the obstacle. In particular, these factors influence the wave characteristics in the neighborhood of the branch point of the shocks (the point C in Fig. 1). Later, it will be important to have sufficiently simple computational relationships characterizing the mutual influence of the parameters at the vertices of the angular zones converging at a triple point (Fig. 2).

The analysis of the triple shock configurations can be reduced to solving a sufficiently complex transcendental equation in the general case [1]. Local utilization of such a procedure, especially as a boundary condition, often is fraught with great difficulties. It is possible to construct an explicit solution in the neighborhood of a triple point in a hypersonic approximation. Writing this solution analytically is simple if we limit ourselves to a quadratic expansion in the two parameters 1/M and $(k-1)$, where M is the freestream Mach number.

If three shock-front generators converge at one point, then one part of the freestream undergoes a single compression on the shock front and the other passes through two shocks. The resultant effect of these actions is characterized by identical magnifications of the pressures. When all the waves have a finite intensity, the wave in the stream with single compression will be stronger near the normal shock. This is the wave N in Fig. 2. The following notation are used in Fig. 2: S is the incident shock, R is the reflected shock, N is the strong shock, and T is the contact discontinuity.

The conservation laws yield the following system of equations in the neighborhood of the triple point:

$$\begin{aligned} &\operatorname{tg}\delta_3 = P(M,\ p_3/p);\ \operatorname{tg}\delta_1 = P(M,\ p_1/p);\\ &\operatorname{tg}\delta_2 = P(M_1,\ p_2/p_1);\quad M_1^2 = R(M,\ p_1/p), \end{aligned} \qquad (2.1)$$

where δ is the angle of stream deflection at the shock front, and the subscripts 1, 2, and 3 correspond to the domain numbers in Fig. 2. The functions P and R can be considered known if the equation of state of the gas is given. In the case of an ideal gas with constant specific heats these functions are

$$P(\mathrm{M}, z) = \frac{z-1}{1+k\mathrm{M}^2-z}\left(\frac{\frac{2k\mathrm{M}^2}{k+1}}{z+\frac{k-1}{k+1}}-1\right)^{1/2};$$
$$R(\mathrm{M}, z) = \frac{\mathrm{M}^2\left(\frac{k+1}{k-1}z+1\right)-\frac{2}{k-1}(z^2-1)}{z\left(z+\frac{k+1}{k-1}\right)}. \tag{2.2}$$

The following conditions are satisfied on the contact discontinuity:

$$p_2 = p_3;\ \delta_3 - \delta_1 + \delta_2 = 0. \tag{2.3}$$

Since one of the shocks is ordinarily strong, and almost normal, then a logical simplification of the computational relations is linearization with respect to a triple configuration with one normal shock [2, 3].

If the shock N is normal, then the parameters in domain 3 are determined independently: $\delta_3 = 0$, p_3/p is a known function of M and k, when the equation of state of the gas is given. For an ideal gas

$$p_3/p = [2k/(k+1)]\mathrm{M}^2 - (k-1)/(k+1).$$

In this case condition (2.3) can be rewritten as follows:

$$-\delta_1 + \delta_2 = 0; \tag{2.4}$$
$$p_1/p = (p_3/p)p_1/p_2. \tag{2.5}$$

Substituting the appropriate expressions for the angles of stream deflection on the shock fronts into (2.4), we obtain

$$\mathrm{arctg}P(\mathrm{M},\ p_1/p) - \mathrm{arctg}P(\mathrm{M}_1,\ p_2/p_1) = 0.$$

In combination with the last relationship in the system (2.1) and condition (2.5), this expression yields a transcendental equation for the pressure p_1 between the fronts of the bifurcated shocks S and R in the general case (see Fig. 2). For an ideal gas with constant specific heats the equation will be algebraic and in the form

$$\sum_{n=0}^{6} K_n(\mathrm{M}, k)\left(\frac{p_1}{p_2}\right)^n = 0. \tag{2.6}$$

For high numbers M its approximate solution can be found as a polynomial in powers of 1/M:

$$p_1/p_2 = a + b/\mathrm{M} + c/\mathrm{M}^2. \tag{2.7}$$

Retaining quantities up to second order in the expansions of the coefficients k_n, we obtain after simple manipulations

$$\sum_{n=0}^{4}\left(a_n + \frac{c_n}{\mathrm{M}^2}\right)\left(\frac{p_1}{p_2}\right)^n = 0, \tag{2.8}$$

where the coefficients a_n and c_n depend only on the ratio of the specific heats. Equation (2.8) is obtained after reduction of the intermediate relation by $(p_1/p_2)^2$, which eliminates the second root $p_1/p_2 = 0$ of (2.6). Substituting (2.7) into (2.8), we again discard higher-order terms and collect the rest in powers of 1/M. Equating the coefficients of powers of 1/M to zero in order to find the a, b, c in (2.7), we find the following relationships:

$$\sum_{n=1}^{4} a_n a^{n-1} = 0; \quad b = 0; \quad c = -\frac{\sum_{n=0}^{4} c_n a^n}{\sum_{n=1}^{4} a_n a^{n-1}}.$$

For the sake of simplicity, we seek the finite relationships a and c in the form of power-law expansions in the quantity $(k-1)$ and retain the first three members. Consequently, we find

$$a = 0{,}25(k-1) - 0{,}5\,(k-1)^2;\ c = [4 + 2(k-1) - 7(k-1)^2]/2(k-1). \tag{2.9}$$

We assume that the angle δ_3 in the jet triple shock configuration is small (the shock N is almost normal) and the flow parameters between the shock fronts differ slightly from the corresponding parameters in a configuration with one normal shock; then

$$p_1 = p_{10} + \Delta p_1;\ p_2 = p_{20} + \Delta p_2;\ M_1 = M_{10} + \Delta M_1;$$
$$\delta_2 = \delta_0 + \Delta\delta_2;\ \delta_1 = \delta_0 + \Delta\delta_1 (\delta_{20} = \delta_{10} = \delta_0).$$

Let us introduce the following notation for the derivatives of the function (2.2):

$$P_1(M, z) = \frac{\partial P}{\partial (M^2)} = \frac{k^2}{k+1}\frac{P(z+1-M^2)}{(1+kM^2-z)\left(\frac{2k}{k+1}M^2 - z - \frac{k-1}{k+1}\right)},$$
$$P_2(M, z) = \frac{\partial P}{\partial z} = P\left(\frac{1}{z-1} + \frac{1}{1+kM^2-z} - \frac{0.5}{z+\frac{k-1}{k+1}} - \frac{0.5}{\frac{2k}{k+1}M^2 - z - \frac{k-1}{k+1}}\right); \tag{2.10}$$
$$R_2(M, z) = \frac{\partial R}{\partial z} = -\frac{\left(M^2 + \frac{2}{k-1}\right)\left[\frac{k+1}{k-1}(z^2+1) + 2z\right]}{z^2\left(z + \frac{k+1}{k-1}\right)^2}.$$

We find to first-order accuracy the following from the second condition in (2.3):

$$\Delta p_1/p = \gamma\delta, \tag{2.11}$$

where γ is a function of M and k determined from an analysis of a triple configuration with one normal compression shock:

$$\gamma = \left\{\cos^2\delta_0\left[P_2\left(M, \frac{p_{10}}{p}\right) - P\left(M_{10}, \frac{p}{p_{10}}\right)R_2\left(M, \frac{p_{10}}{p}\right) + P_2\left(M_{10}, \frac{p_{20}}{p_{10}}\right)\left(\frac{p}{p_{10}}\right)^2\frac{p_{20}}{p}\right\}^{-1}; \tag{2.12}$$

P_1, P_2, R_2 are calculated by means of (2.10) by substituting the appropriate M and z. It is possible to proceed substantially toward lesser values of M if the linear term in 1/M is retained in (2.7) and the coefficients a, b, and c are determined by sampling by approximating the results of exact computations. The following dependences are recommended:

$$a = -0.0175 + 0{,}3793(k-1) - 0.1727(k-1)^2;$$
$$b = 1.2382 - 1.2579(k-1) + 0.3813(k-1)^2;$$
$$c = -0{,}4044 + 0.2830(k-1) + 0.0324(k-1)^2.$$

If p_1/p_2 is determined by (2.7), then a simple dependence can be obtained for γ. After substituting the expressions for the quantities in the right side of (2.12), we carry out an expansion in 1/M and retain the first three terms. Consequently, we obtain a relationship analogous to (2.7) for the quantity γ/M^2. It hence follows that

$$\gamma = A + BM + CM^2,$$

where A, B, C depend only on k. These coefficients are approximated well by

$$A = -1.7901 + 13.2841(k-1) - 13.2702(k-1)^2;$$
$$B = 1.6318 - 10.3203(k-1) + 9.8089(k-1)^2;$$
$$C = 0.1315 + 2.3768(k-1) - 1.6327(k-1)^2.$$

The results of computing an arbitrary triple shock configuration by means of the approximate method elucidated agree satisfactorily with the results of an exact computation for values of δ_3 up to 10-12°. The discrepancy in the relative pressures is less than 8% for M > 2.

Application of the approximate dependences presented reduces the computation of the parameters in triple shock configurations to the execution of elementary calculations.

§3. Phenomena in the neighborhood of the jet boundary, near the hanging shock front on both sides, and in the shock bifurcation zone are of a quite definite nonuniform character. The following method, approved by numerous comparisons with the results of computations and the data of experiments in a broad range of initial parameters [4], can be recommended for an approximate analytical description of the flows in these domains.

Let us assume that an n-parameter family of curves $f(x, y, a_1, a_2, \ldots, a_n) = 0$ is known such that a curve of this family can be selected for any escape mode, which approximates the jet boundary well enough, i.e., the question of finding the boundary reduces to determining n values of the parameters a_i for specific escape conditions. If the jet boundary is simulated by a solid wall to be graphic, then the hanging shock can be treated as the bow wave originating in the supersonic flow around a concave surface. The higher the Mach number in this stream, the closer does such a wave approach the streamlined surface. On this basis, certain authors used the limit hypersonic approximation: it was assumed that the hanging shock coincides with the jet boundary. For finite, but large Mach numbers ahead of the hanging shock, its generator differs slightly in shape from the line mapping the boundary and can be obtained geometrically from it by a relatively small deformation. Such a deformation can approximately be carried out analytically because of a change in the parameters in the structural dependence governing the shape of the jet boundary, i.e., the problem of defining the shape of the hanging shock reduces to selecting a specific curve from the same n-parameter family $f(x, y, b_1, b_2, \ldots, b_n) = 0$. Here the free parameters of the family are denoted by b_i $(i=1,2, \ldots, n)$ in order to separate the second selection procedure from the first. The number 2n equals the number of conditions which are successfully formulated sufficiently simply for the boundaries and the hanging shock.

Let us turn to possible formulations of these conditions. Part of them are successfully formulated exactly and simply; the rest yield only to a more or less approximate description. An approximate method to find the position of the central compression shock was considered above. There exist many other approximate and semiempirical methods of determining this quantity with good accuracy. Below we shall consider the coordinate x_s known. The diameter of the central shock (the coordinate y_s) is considerably more difficult to subject to calculation. In substance, there are no reliable methods of finding this quantity. Hence, we shall henceforth consider y_s unknown together with the parameters governing the shock boundary and arc. As yet we assume that all the flow parameters are computed successfully in the neighborhood of the shock-front branch point.

The hanging shock is generated at interior points of the stream in the form of a zero intensity wave as a result of the intersection of characteristics reflected from the boundary. On a certain section it can be considered to coincide with the envelope of the characteristics mentioned, where the first reflected characteristics already intersect, since the initial radius of curvature of the boundary differs from zero [5]. Starting from these considerations, the point of hanging shock generation and its initial slope can be found. Therefore, there is a possibility of forming the following five evident conditions which the equations of the boundary and shock generators should satisfy: 1) the boundary passes through the point (0.1); 2) its slope at this point is ϑ_H; 3) the slope of the shock is known at $x = x_s$; 4) the coordinates of the point of hanging shock generation (x_0, y_0) can be calculated; 5) the initial slope of the hanging shock is to be determined.

Finally, by using the integral mass conservation law for the section in which the central shock is located (see Fig. 1), the radius of the boundary in this section (the coordinate y_3) can be determined under certain simplifying assumptions. This result is used as condition 6.

Further, two approximate conditions can be obtained for an examination of the flow in the neighborhood of the point M (Fig. 3), where the tangent to the hanging shock generator is parallel to the axis of symmetry. Let us consider the shock to be so weak on the section OM that its front is practically indistinguishable from the envelope of the family of characteristics reflected from the boundary, which are themselves rectilinear. Then the characteristic arriving at the point M from the boundary will coincide with the tangent to the hanging shock at this point and is therefore parallel to the axis of symmetry. Condition 7 hence follows: the ordinate of the point M (y_m) equals the ordinate of that point on the boundary in which the slope of the tangent equals the known Mach angle α_H. Finally, we have condition 8: the mass flow rates of gas through the segments M_1M and MM_2 are equal (see Fig. 3). The discharge through the section MM_2 can be determined in the same approximation as through the section CM_3, and the distribution of all the parameters along the rectilinear characteristic M_1M is known, in particular, the mass flow rate can be calculated.

Let us examine two versions of solving the problem: taking account of conditions 7 and 8 and without taking these conditions into account. In the first case, a four-parameter family of curves can be selected to approximate the boundary and the hanging shock (n = 4), and in the second case, a three-parameter family (n = 3).

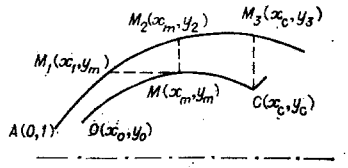

Fig. 3

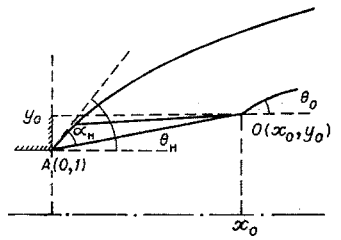

Fig. 4

Let us proceed to a specific realization of the scheme designated. Writing the first three equations is evident. Let us examine the formulated conditions in the above-mentioned order by starting with the fourth.

Condition 4. The coordinates (x_0, y_0) of the point can be expressed in terms of the radius of curvature R_H of the initial element of the jet boundary under the assumption that the characteristics are practically rectilinear up to the point of intersection (Fig. 4).

A simple approximate formula for R_H can be obtained from the equation of motion in projections on the normal to the streamline with the continuity equation taken into account:

$$\rho w^2/R = -\partial p/\partial n, \quad \partial\vartheta/\partial n + (1/\rho w)\partial\rho w/\partial s = -\sin\vartheta/y,$$

where R is the local radius of curvature; s and n are the distance along the streamline and its normal. Since ρw = const along the boundary, we obtain from the last equations

$$\rho w^2/R = (\sin\vartheta/y)\partial p/\partial\vartheta.$$

The derivative $\partial p/\partial\vartheta$ is evaluated along the normal to the boundary. A change in pressure in the elementary compression wave reflected from the boundary is calculated approximately by means of the plane theory of small disturbances. The flow in the neighborhood of the boundary is irrotational; hence

$$dp \approx (\rho w^2/\sqrt{M^2-1})d\vartheta.$$

Therefore,

$$R_H = \frac{\sqrt{M_H^2-1}}{\sin\vartheta_H} = \frac{\operatorname{ctg}\alpha_H}{\sin\vartheta_H}, \tag{3.1}$$

where α_H is the Mach angle; ϑ_H is the initial slope of the boundary generator to the jet axis. The approximate formula (3.1) yields completely satisfactory agreement with the results of exact calculations [5]. According to (3.1) and Fig. 4, the coordinates of the point of hanging shock generation are determined by the formulas

$$x_0 = (\cos\alpha_H/\sin\vartheta_H)\cos(\vartheta_H - \alpha_H); \quad y_0 = 1 + (\cos\alpha_H/\sin\vartheta_H)\sin(\vartheta_H - \alpha_H).$$

Condition 5. The parameters in the neighborhood of the triple point possess great sensitivity to the change in the magnitude of the initial slope θ_0 of the hanging shock to the jet axis. The arc of the hanging shock has considerable extent; hence, small errors in determining the angle θ_0 can be the source of considerable errors at the end of this arc. Let us calculate the magnitude of the increment in the characteristic angle $(\vartheta - \alpha)$ during displacement along the last characteristic which converges with the sharp nozzle edge. In the neighborhood of this edge, the derivatives of the gasdynamic quantities along the first family characteristic in the rarefaction-wave domain are very much greater in absolute value than the same quantities in the direction of the second family characteristics. Hence, the compatibility relationship along the first family characteristic is satisfied approximately in all directions in the same form as for plane flows:

$$d\vartheta + \{\cos^2\alpha/[(k-1)/2 + \sin^2\alpha]\}d\alpha = 0. \tag{3.2}$$

In particular, this relationship is valid along the initial element of the boundary characteristic on which the exact relationship for the second family characteristics is satisfied:

$$d\vartheta - \{\cos^2\alpha/[(k-1)/2 + \sin^2\alpha]\}d\alpha - \sin\alpha\sin\vartheta dl = 0, \tag{3.3}$$

where dl is the element of displacement along the characteristic mentioned. It follows from (3.2) and (3.3) that

$$d(\vartheta - \alpha)/dl = [(k+1)/4]\sin\alpha\cdot\sin\vartheta/\cos^2\alpha.$$

This latter formula affords a possibility of introducing a linear correction to the magnitude of the angle

$$\vartheta_0 = \vartheta_н - \alpha_н + [d(\vartheta - \alpha)/dl]_н l = \vartheta_н - \alpha_н + [(k+1)/4]\mathrm{tg}\alpha_н.$$

The computations presented showed that taking account of such a correction is one of the fundamental hypotheses for raising the accuracy of determining the shock-configuration parameters in a jet.

Condition 6. The mass flow rate through an annular section CM_3 (see Fig. 3) is

$$Q = 2\pi\int_{y_s}^{y_3}\rho u y dy, \tag{3.4}$$

where u is the axial velocity component. There are no sharp peaks of the gasdynamic parameters between the boundaries and the hanging shock, and all the quantities vary sufficiently smoothly across the domain. The mass flux density ρu in the section CM_3 is approximated by a linear function in y. We note the parameters at the point C between the bifurcated shock fronts by the subscript 1. Under such assumptions

$$\rho u \approx \rho_1 u_1 + [(\rho_н u_н - \rho_1 u_1)/(y_3 - y_s)](y - y_s).$$

After evaluating the integral in (3.4), the result is reduced to the form $Q = 2\pi[\rho_1 u_1(y_3 + y_S) + (\rho_H u_S - \rho_1 u_1)\cdot(y_S + 2y_3)/3](y_3 - y_S)$. The discharge Q equals the discharge in the jet after subtraction of the gas discharge passing through the central shock. Since the section under consideration is usually located near the maximum jet section, the slope of the boundary to the jet axis at the point M_3 is a small quantity and at least for u_H it is possible to set $u_H = w_H\cos\vartheta_H \approx w_H$.

Conditions 7 and 8. It is necessary to set $y = \mathrm{const} = y_m$ and, therefore, $\vartheta \equiv \alpha$, along the second family characteristic M_1M, where α is the Mach angle ($\sin\alpha = 1/M$). Selecting the Mach number M as the argument, we obtain from (1.6)

$$dx/d\mathrm{M} = \{2 + [(k-3)/2]\mathrm{M}^2\}/\{1 + [(k-1)/2]\mathrm{M}^2\} = 1/K.$$

Further calculations can be performed exactly; however, they are unjustifiedly tedious. The approximations

$$K \approx \mathrm{const} = K_н;\ \rho a \approx \rho_н a_н[1 + (d\ln\rho a/d\mathrm{M})_н(\mathrm{M} - \mathrm{M}_н)];$$
$$\mathrm{M} - \mathrm{M}_н \approx K_н(x - x_s)$$

along the characteristic M_1M (a is the speed of sound) and

$$\rho u \approx \rho_н u_н[1 - (d\ln\rho u/dy)_н(y - y_2)]$$

along the line MM_2 can be used without substantial loss in accuracy. Substituting these expressions in the equality of the discharges ($v \equiv a$ on M_1M), we obtain an equation connecting the coordinates of the points on the two desired curves after simple manipulations:

$$2[1 + (d\ln\overline{\rho a}/d\mathrm{M})_н K_н(x_m - x_1)](x_m - x_1) =$$
$$= \mathrm{M}_н(y_2 - y_m)[y_2 - y_m - (d\ln\rho w/d\mathrm{M})_н K_н(x_m - x_1)(y_2 - 2y_m)/3].$$

Let us make the following recommendations relative to the selection of the parametric families of the curves approximating the boundary and the arc of the hanging shock.

In the case of the four-parameter problem, the fact that the boundary is often successfully mapped completely satisfactorily by the arc of a circle, i.e., the curvature along the boundary should be a slightly varying

function of the arc length or coordinate, say y, can be taken as a priori information. In a first approximation this function can be represented as a linear dependence $a_1 - a_2^2 y$. On the other hand, for relatively small angles we consider the curvature approximately equal to d^2y/dx^2. We then obtain the equation

$$d^2y/dx^2 = a_1 - a_2^2 y,$$

whose general integral

$$y = a_3 \sin(a_2 x + a_4) + a_1/a_2^2 \tag{3.5}$$

yields a four-parameter representation of the boundary (a_1, a_2, a_3, a_4 are arbitrary parameters). The curves of the family (3.5) can approximate the boundary and the shock well in practically any escape mode. However, substituting the function (3.5) into the eight conditions formulated above results in a quite complicated system of transcendental equations. For fast approximate computations it is best to use the three-parameter model. In the case of the three-parameter problem the structural formula for the family of curves is obtained at once from the solution in a near-axis approximation in the form of (1.3), from which there follows that all the isobars and particularly the boundary are described by an equation for second-order curves in the form

$$y = \sqrt{a_1 + a_2 x + a_3 x^2}, \tag{3.6}$$

i.e., the boundary and wave front are approximated by arcs of ellipses in this approximation.

Let us especially consider the question of determining the radius of the central shock y_s. For the sake of simplicity, let us examine the final result in the case of a three-parameter approximation of the form (3.6).

A tendency to stream equilibration in the direction of the jet axis always exists in a jet flow. The slopes of the velocity vector to the jet axis already become small after the first system of shocks. A contact discontinuity converging with the contour of the central shock, which can be considered a normal compression shock in a first approximation, also possesses this property. Then the initial slope of the contact discontinuity equals zero, and the stream through the shock front can be considered one-dimensional.

Let us represent the following as the second approximation: the velocity vector w ahead of the triple point C forms a small angle ε with the axis of symmetry, the angle of the incident shock with this vector varies by a small quantity $\Delta\omega$, the central shock curves, and the initial element of the contact discontinuity remains parallel to the axis. Therefore, in a second approximation $\varepsilon - \delta_1 + \delta_2 = 0$, where δ_1 and δ_2 are the angles of stream rotation on the incident and reflected shocks, respectively.

Let us use the formula (2.11) obtained above. Then

$$\Delta p_\perp/p = \gamma(M)\varepsilon, \quad \Delta\omega = (k+1)\gamma(M)\varepsilon/2kM^2\sin 2\omega. \tag{3.7}$$

Let us assume the flow through the central shock contour to be one-dimensional in a stream tube passing through the central shock contour. Hence

$$\varepsilon \approx dy/dx = (d\ln y/dM)(dM/dx)y = [\beta(M)/\eta(M)]y, \tag{3.8}$$

where

$$\beta(M) = [\eta(M)/2x^1(M)]d\ln q(M)/dM;$$
$$\eta(M) = 1 - (k+1)\gamma(M)/2kM^2\sin 2\omega.$$

Here q(M) is a tabulated gasdynamic discharge function, and x(M) is a function characterizing the Mach number distribution along the jet axis. On the basis of (3.7) and (3.8)

$$\theta_s = \omega + \Delta\theta = \omega - \beta y_s.$$

Substituting the value of θ_S in the conditions 3-5, we find the radius of the central compression shock

$$y_s = \frac{1}{2}\left(1 - \beta\frac{x_s - x_\theta}{\cos^2\omega}\right)^{-1}\left\{\left[(x_s - x_0)^2\operatorname{tg}^2\omega + 4y_0\left(1 - \beta\frac{x_s - x_0}{\cos^2\omega}\right)(y_0 + (x_s - x_0)\operatorname{tg}\theta_0)\right]^{1/2} - (x_s - x_0)\operatorname{tg}\omega\right\}. \tag{3.9}$$

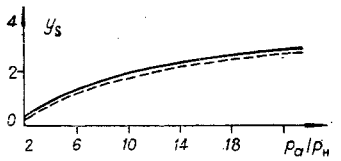

Fig. 5

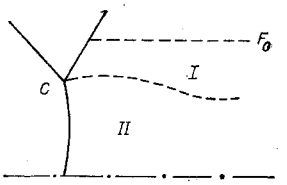

Fig. 6

Numerous computations were performed of the shock configurations for underexpanded jets in a broad range of initial parameter values. Results of the computations were compared with published results of numerical computations and experimental measurements. Presented in Fig. 5 is a comparison between a computation using (3.9) and the results of experiments [5] (the solid and dashed lines, respectively) for $M_a = 1.5$, $k = 1.4$.

Analogous results have been obtained for other values of the initial parameters:

$$1 \leqslant M_a \leqslant 5,\ 2 \leqslant p_a/p_н \leqslant 100.$$

An estimate made of the influence of the possible assumptions on the magnitude of the radius of the central shock showed that replacing it by a normal shock ($\beta = 0$) induces an error on the order of 20-30% in y_s. Displacement of the point of hanging shock generation to the nozzle edge changes the value of y_s by 30-40%. But the greatest error is associated with determining the initial slope of the hanging shock: equating θ_0 to the angle $\vartheta_н - \alpha_н$ changes y_s by 50-70%. The errors mentioned can hence appear in one direction, i.e., do not cancel each other.

§4. For the sake of completeness of analysis of the question about a free jet, let us examine the possible method of describing the flow in a gas jet passing through a central compression shock, particularly the determination of the shape of the contact discontinuity.

Let a certain stream tube with the cross-sectional area $F_0 \approx$ const (Fig. 6) exist such that the flow on its boundary is already practically independent of the shape of the contact discontinuity. Let us consider the generators of this surface rectilinear and parallel to the axis of jet symmetry. Let us partition the flow in the stream tube into two parts: a one-dimensional flow within the stream tube which rests on the central shock contour (the domain II in Fig. 6) and an outer supersonic flow in the annular domain I, where the one-dimensional description of the motion turns out to be inadequate. If f is the cross-sectional area of domain II, then a change in pressure along the contact discontinuity from this domain is written as

$$dp_2 = (dp/df)df.$$

The change in pressure from the supersonic domain side I is determined by two causes: first, for each rotation of the boundary through a small angle $d\vartheta$ elementary compression or rarefaction waves stand off from the boundary in conformity with the direction of rotation; secondly, effective broadening or compression of the whole stream occurs because of the change in cross-sectional area of the annular stream tube. These effects can appear in one or the opposite directions. The resultant pressure change from the outer flow is representable as

$$dp_1 = (\partial p/\partial F)dF + (\partial p/\partial\vartheta)d\vartheta.$$

The pressure continuity condition on the contact surface $dp_1 = dp_2$ can be written as

$$(dp/df)df = (\partial p/\partial F)dF + (\partial p/\partial\vartheta)d\vartheta. \tag{4.1}$$

According to one-dimensional theory

$$\frac{dp}{df} = -\frac{1}{f}\frac{kpM_2^2}{M_2^2-1};\quad \frac{\partial p}{\partial F} = -\frac{1}{F}\frac{kpM_1^2}{M_1^2-1}.$$

According to the theory of simple waves

$$\frac{\partial p}{\partial \vartheta} = \frac{kM_1^2 p}{\sqrt{M_1^2 - 1}}.$$

Evidently,

$$f = \pi y^2;\ F = F_0 - f.$$

After the substitutions mentioned, (4.1) becomes

$$d\vartheta + \left(\frac{y}{F_0 - f} \frac{2\pi}{\sqrt{M_s^2 - 1}} + \frac{\sqrt{M_2^2 - 1}}{M_1^2 - 1} \frac{M_2^2}{M_1^2} \frac{2}{y} \right) dy = 0. \tag{4.2}$$

The radius of the stream tube II is a relatively slightly varying quantity. Hence, the first member in the parentheses is a finite, almost constant value. The second member can grow without limit as $M_2 \to 1$, but this member is much less than the first in sections where M_2 is considerably less than one, since $M_2^2/M_1^2 \ll 1$. Therefore, the contribution of the second member must be taken into account only near the critical section, i.e., in the second member M_2 can be replaced by its asymptotic expression as $M_2 \to 1$, as follows from the differential relationship between the section area and the Mach number in a one-dimensional stream:

$$\frac{df}{f} = \frac{M_2^2 - 1}{M_2 \left(1 - \frac{k-1}{2} M_2^2 \right)} dM_2. \tag{4.3}$$

We hence obtain as $M_2 \to 1$

$$(y - y_*)/y \approx [2/(k+1)](M_2 - 1)^2,$$

where y_* is the radius of the critical section,

$$\frac{y_*}{y_s} = \left(\frac{1 + \frac{k-1}{2} M_{2s}^2}{\frac{k+1}{2}} \right)^{(k+1)/4(k-1)},$$

and M_{2s} is the Mach number behind the central shock. Let us introduce the notation $\eta = (y - y_*)/y_*$. Then $M_2 \approx 1 \mp \sqrt{[(k+1)/2]\eta}$ (the minus sign should be taken for the subsonic section and the plus sign for the supersonic section of the jet). According to the above, we can put $M_1 - 1 \approx \sqrt{[(k+1)/2]\eta}$ in (4.2) in the whole subsonic section. After integrating with the condition $\vartheta = 0$ for $\eta = 0$ (in the critical section), we obtain

$$\vartheta = 2 \left(\frac{\sqrt{M_{2s}^2 - 1}}{\sqrt{k+1}\, y_s} \frac{2\sqrt{2}}{M_{2s}^2} - \frac{y_s}{F_0 - f} \frac{\pi \sqrt{\eta}}{\sqrt{M_{2s}^2 - 1}} \right) y_* \sqrt{\eta} \tag{4.4}$$

(the slightly varying quantities in the parentheses are replaced by their values in the initial section). It follows from (4.4) that $\vartheta = 0$ (except the minimum section) and in the section where

$$\sqrt{\eta} = \frac{2\sqrt{2}}{\sqrt{k+1}} \frac{M_{2s}^2 - 1}{\pi y_s M_{2s}^2} (F_0 - f).$$

Here the maximum of the jet cross-sectional area evidently holds. However, it is still impossible to determine the radius of this section by means of this last formula, since F_0 is an unknown constant. To determine it, it is necessary to know the initial value of the slope of the contact discontinuity ϑ_s, in (4.4) and above $\vartheta_s = 0$. This quantity can be determined more exactly in the framework of the reasoning used. Let us clarify this possibility without going into detail, since ϑ_s for a free jet is henceforth of no interest.

The central shock in a free jet is a curvilinear surface turned convexly downstream (Fig. 7). The tendency for equilibration of the velocity directions along the axis of symmetry in a jet has already been noted. If it is assumed that the equilibration is achieved completely behind the central shock, then the flow in II will be an isobaric vortex stream parallel to the axis. The angle of stream rotation on the wave front at each point of the front is then equal to the slope of the velocity vector ϑ to the axis ahead of the front, i.e.,

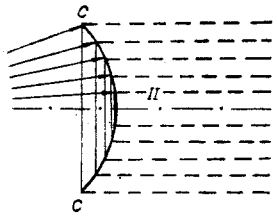

Fig. 7

$$\vartheta \approx \frac{\frac{p_2}{p} - 1}{1 + kM^2 - \frac{p_2}{p}} \sqrt{\frac{\frac{2k}{k+1} M^2}{\frac{p_2}{p} + \frac{k-1}{k+1}} - 1} \qquad (4.5)$$

according to the known formula for shocks (2.1). Here the tangent is replaced by the argument; p_2 is the constant pressure behind the front; p is the variable pressure in the nonuniform stream ahead of the front, which is a known function of M (isentropic coupling), i.e., $\vartheta = \Theta(M)$ because of (4.5), where Θ is a known function. The flow ahead of the shock front will be examined in a one-dimensional approximation. Then

$$\vartheta = dy/dx = (y/2)(d \ln f/dM)dM/dx.$$

In the one-dimensional stream d ln f/dM is a known function of M, i.e., $(1/2)d\ln f/dM = \varphi(M)$. From the last two equations

$$dM/dx = \Theta(M)/y\varphi(M). \qquad (4.6)$$

Let $\partial y/\partial x$ be the derivative along the wave front and ω the slope of the front to the velocity vector ahead of the front; then

$$\partial y/\partial x = \operatorname{tg}(\omega - \vartheta) = \varepsilon(M),$$

where $\varepsilon(M)$ is a known function. Hence and from (4.6)

$$\partial \ln y/\partial M = \varepsilon(M)\varphi(M)/\Theta(M).$$

This latter equality determines y(M), and M(x) is found from (4.1), i.e., the Mach number distribution law before the wave front. Such a distribution differs from that given in the incoming jet. Hence, complete equilibration of the velocity directions is impossible and is achieved just as much as the existing distribution M(x) in the jet ahead of the shock admits. Near the jet axis $\vartheta \sim y$. Taking the dependence $\vartheta = ay$ behind the shock front will be the simplest refinement of the computational scheme (a is a constant). If it is considered that $\vartheta \neq 0$, $\vartheta = ay$ for all the previous assumptions, then $\vartheta - ay$ must be written in place of ϑ and the result of integrating the relation (4.6) will contain the parameter a: $M = M(x, a)$. Now a must be selected such that the dependence $M(x, a)$ will approximate the given dependence optimally in some sense. This defines $\vartheta_S = ay_S$. All the operations mentioned are realized simply, since the range of variation of the Mach numbers under consideration is quite small and it is possible to limit oneself to the first terms of the expansion everywhere.

Let us consider model constructions for restricted jets interacting with obstacles by considering the obstacle such that it does not spoil the axial symmetry.

§5. As before, the problem of determining the position of the central compression shock remains one of the fundamental questions. Now the coordinate x_S depends not only on the counterpressure, but primarily on the position and shape of the obstacle. There are still no convenient and simple methods of determining these quantities. Experimental investigations are not subject to sufficient generalization, and numerical methods are fraught with major difficulties in their realization.

Presented in Fig. 8 is a stream scheme in the case of an underexpanded jet ($p_a/p_H > 1$), impinging on an obstacle, where OC is the hanging, CB the reflected, and CC the central compression shock; CE is the contact discontinuity; and ABD is the jet boundary; the solid lines are the shock fronts and the dashes denote contact discontinuities. Up to the last system of compression shocks (CC and CB) the stream in front of the face side of the obstacle 2 coincides with the flow in a free jet with the same parameters in the nozzle exit section 1. The solution for this part of the stream is assumed known.

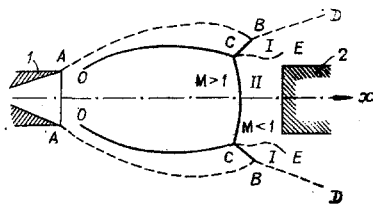

Fig. 8

The stream behind the system of compression shocks CC and CB can be separated into two domains: II is the flow domain behind the central compression shock between the contact discontinuity and the body surface, and I the domain of the peripheral stream external with respect to II.

If the shape of the contact discontinuity has been found, then the computation of the flow in the peripheral stream domain reduces to the problem of the nonuniform flow around a certain body with one attached shock.

An approximate method is proposed, based on the linear approximation of the velocity dependence on the pressure along a streamline, to determine the flow in domain II. Such an approach has been used in external flow problems [6, 7].

The linear approximation permits integration of the system of gasdynamic equations for an inviscid non-heat-conducting gas. A simple connection is hence obtained between the kinematic flow parameters (kinematic integral), which affords the possibility of finding the position of the triple point and the shape of the contact discontinuity without solving the problem as a whole [8].

The pressure dependence of the velocity is written as

$$w = Ap + B,$$

where A and B are functions of just one variable, the stream function ψ, which is determined by the relationship

$$d\psi/\rho w = y\cos\vartheta dy - y\sin\vartheta dx. \tag{5.1}$$

By virtue of the approximation used, ρw is also a function of just the one variable ψ; hence, we have a total differential of some function in the left side of (5.1). The condition that a total differential is on the right is written as

$$\partial(y\cos\vartheta)/\partial x + \partial(y\sin\vartheta)/\partial y = 0.$$

Hence

$$x = y\sin\vartheta\ln\operatorname{tg}(\vartheta/2) + f(y\sin\vartheta), \tag{5.2}$$

where $f(y\sin\vartheta)$ is an arbitrary function of its argument, determined from the condition of impermeability on the body surface. For fundamental obstacle shapes the expression for it is written explicitly.

The streamline equation can be integrated in the presence of the kinematic integral (5.2). The result is obtained in finite form. Therefore, the equation of the line of the contact discontinuity can be determined as a streamline converging with the contour of the central compression shock.

Since the position of the central compression shock is unknown in advance, it is considered that the triple point can occupy any position on the hanging compression shock. Knowledge of the flow field in a free jet with the same parameters in the nozzle exit section as in the jet impinging on the obstacle yields the equation of an arc of the hanging shock and the stream parameters in front of it. All the stream parameters behind the triple point, including even the slope of the velocity vector to the axis of symmetry, can be determined for each point of this shock by means of the relations for the triple shock configuration. Therefore, a dependence of this angle on the axial coordinate $\vartheta = \Theta_1(x)$ is obtained from a computation of the free jet.

For a given obstacle position, the slope of the velocity vector behind the triple point can be found for all points of the hanging shock and from a computation of domain II. Along the contour of a body of given shape,

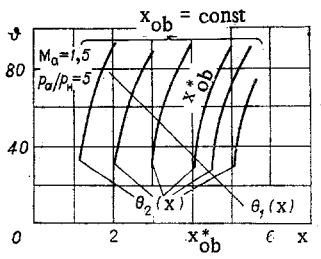

Fig. 9

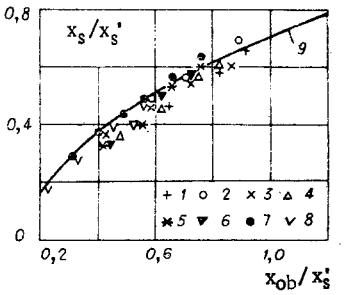

Fig. 10

the dependence $\vartheta = \Theta(y)$, which determines the form of the arbitrary function $f(y \sin \vartheta)$, is considered known. For each point corresponding to the equation of the hanging shock, ϑ is found by means of the relationship (5.2), i.e., the same dependence of the slope of the velocity vector behind the triple point is determined, but from the solution taking account of the condition on the body $\vartheta = \Theta_2(x)$. The position of the triple point is determined by the intersection between the curves $\vartheta = \Theta_1(x)$; $\vartheta = \Theta_2(x)$.

Results of a computation for one of the specific cases when the parameters in the nozzle exit section are constant and the spacing between the nozzle and the obstacle taken on a number of values are presented as an illustration in Fig. 9. There is one curve of the dependence $\vartheta = \Theta_1(x)$ and a set of curves of the dependence $\vartheta = \Theta_2(x)$, where each curve of this set corresponds to a definite position of the obstacle $x = x_{ob}$. The position of the triple point for each value of x_{ob} is found from the intersection of the appropriate curve $\vartheta = \Theta_2(x)$ with the curve $\vartheta = \Theta_1(x)$.

Positions of the central shock (the triple point) were computed according to the scheme given above for the following range of the governing parameters: $p_a/p_H = 3 - 12$; $M_a = 1 - 3$; $\vartheta_a = 0^0$, $k = 1.4$. The obstacles were taken as infinite planes and cylinders with a flat end face. The spacing between the nozzle and the obstacle did not exceed the length of the initial gasdynamic section of the jet. The stream parameters in a domain which agrees with the flow in a free jet and the equation of an arc of the incident shock were computed by the method elucidated above.

A comparison between the computed data in relative coordinates and the experimental data for jet inflow on a flat infinite obstacle is given in Fig. 10 (values of M: $1 - 1.0$; $2, 3, 4 - 1.5$; $5, 6 - 2.0$; $7, 8 - 3.0$; values of p_a/p_H: $1, 4, 6 - 12$; $2, 8 - 5$; $3, 5, 7 - 8$). The distances between the nozzle and obstacle and the central compression shock x_s are referred to the distance between the nozzle and the central shock x_s' in a free jet. The free jet parameters were taken equal to the parameters of a jet impinging on the obstacle for each point. The experimental data are represented in Fig. 10 as the curve 9 of a generalized dependence [9], valid in the range of governing parameters under consideration (the solid line). Agreement between the computed and experimental data can be considered satisfactory.

§ 6. Stream tubes in the neighborhood of the axis of symmetry of the impinging jet undergo sharp changes in their configuration ahead of the obstacle. A relatively small region of essentially spatial flow can be simulated by a discontinuity in the stream parameters, among which is the cross-sectional area of the tube (Fig. 11). The influence of the obstacle on the fundamental jet flow parameters is studied by using the general conservation laws written down for a conditional discontinuity [10]. In particular, such an approach permits establishment of a connection between the position of the Mach disk in a system of bifurcated shocks and the force of jet action on the obstacle. Approbation of the approach proposed is a confirmation of this connection by means of quantities easily measured in an experiment, as has been done for available data.

Let us write the general conservation laws for the conditional discontinuity:

$$\begin{gathered}\rho_1 w_1 F_1 = \rho_2 w_2 (F_2 - F_{ob});\\ \rho_2 w_2^2 (F_2 - F_{ob}) - \rho_1 w_1^2 F_1 = p_1 F_1 - p_2 (F_2 - F_{ob}) - R';\\ \frac{w_1^2}{2} + \frac{a_1^2}{k-1} = \frac{w_2^2}{2} + \frac{a_2^2}{k-1},\end{gathered} \tag{6.1}$$

where F is the cross-sectional area of the stream tube (F_{ob} is the area of the obstacle). The subscripts 1 and 2 refer to the appropriate checking sections 1–1 and 2–2 in Fig. 11. Let us use the notation

$$R' = R - R'',$$

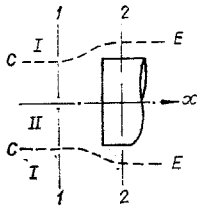

Fig. 11

where R is the reaction of the obstacle, and R" is the axial component of the force acting on the contact discontinuity surface between sections 1 and 2. Let us introduce the dimensionless coefficient β for the force R':

$$R' = \beta\rho_1 w_1^2 F_1. \tag{6.2}$$

Taking account of (6.2), the equation

$$\frac{1+\frac{k-1}{2}M_2^2}{1+\frac{k-1}{2}M_1^2} = \frac{M_1^2}{M_2^2}\frac{(kM_2^2+1)^2}{[kM_1^2(1-\beta)+1]^2},$$

is found from the system (6.1); its solution has the form

$$M_2^2 = 1 - \frac{(k+1)\sqrt{[kM_1^2(1-\beta)+1]^2 - 2(k+1)M_1^2\left(1+\frac{k-1}{2}M_1^2\right)}}{k\sqrt{[kM_1^2(1-\beta)+1]^2 - 2(k+1)M_1^2\left(1+\frac{k-1}{2}M_1^2\right)} + 1 + kM_1^2(1-\beta)}.$$

The sign in front of the radical is selected such that for $w_1 \to 0$; $w_2 \to 0$.

The maximum value of the Mach number ($M_2 = 1$) is achieved when the radicand equals zero. Hence, for the limit mode

$$\beta = \frac{(1-M_1^2)^2}{kM_1^2\left[1+kM_1^2+M_1\sqrt{2(k+1)\left(1+\frac{k-1}{2}M_1^2\right)}\right]},$$

where the sign in front of the radical is selected from the condition $\beta \geq 0$ (the force is $R' \geq 0$ and is directed along the jet axis).

Let us separate the stream in front of the obstacle into exterior I and interior II with respect to the contact discontinuity CE which converges with the contour of the central shock (see Fig. 11). If the pressure from the exterior stream side p can be considered a slightly varying quantity, then

$$R'' \approx p(F_2 - F_1).$$

The shape of the contact discontinuity is such that $p \geq p_1$ (p_1 is the pressure in the interior stream). In estimates, p was taken equal to the lower limit of p_1.

From the conservation laws there follows

$$\frac{p_1}{p_2} = f\frac{M_2}{M_1}\sqrt{\frac{1+\frac{k-1}{2}M_2^2}{1+\frac{k-1}{2}M_1^2}}, \tag{6.3}$$

where $f = (F_2 - F_{ob})/F_1$.

If irreversible losses between the sections 1–1 and 2–2 are neglected, then

$$\frac{p_1}{p_2} = \left(\frac{1+\frac{k-1}{2}M_2^2}{1+\frac{k-1}{2}M_1^2}\right)^{k/(k-1)} \tag{6.4}$$

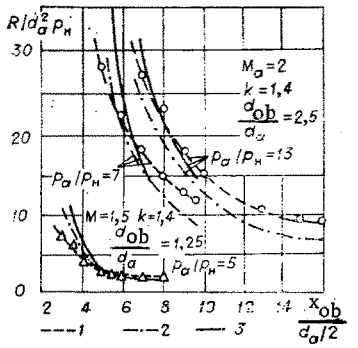

Fig. 12

From (6.3) and (6.4) we find

$$f=\frac{M_1}{M_2}\left(\frac{1+\frac{k-1}{2}M_1^2}{1+\frac{k-1}{2}M_2^2}\right)^{-(k+1)/2(k-1)}.$$

For $M_2 = 1$

$$f=M_1\left(\frac{k+1}{2}\right)^{(k+1)/2(k-1)}\left(1+\frac{k-1}{2}M_1^2\right)^{-(k+1)/2(k-1)}.$$

Finally,

$$R=p_1[F_1(f-1)-F_{ob}]+\beta k p_1 M_1^2 F_1.$$

The flow to the central shock agrees with the flow in a free jet. Hence, to determine the parameters behind the central shock it is sufficient just to know its position.

Let us examine the results of computations in which the values of the central shock coordinate x_s was taken from the experimental data [11]. The flow behind the shock was considered parallel to the axis ($F_1 = F_s$) and the stream parameters in the section 1–1 were assumed equal to the parameters on the jet axis behind a normal compression shock. The results of the computations were compared with data obtained by integration over available experimental points characterizing the pressure distribution on the obstacle surface.

Results are presented in Fig. 12 in the stationary flow case; the curves 1 correspond to the experimental results and curves 2, to the computation by the scheme elucidated above. An analogous correspondence between the results is obtained also for the other initial parameters when the radius of the obstacle is on the order of the radius of the central compression shock.

The position of the Mach disk can be determined by computation also by the method elucidated above. Curves 3 in Fig. 12 correspond to the results of a computation of the body reaction by using computed values of x_s.

§ 7. If the position of the obstacle is such that there is no intersection of the curves $\vartheta = \Theta_1(x)$ and $\vartheta = \Theta_2(x)$ ($x_{ob} > x^*_{ob}$ in Fig. 9), then the solution of the problem can be constructed theoretically: the position of the shock should hence correspond to the greatest achievable distance from the obstacle and the two values $\vartheta = \Theta_1(x_s)$ and $\vartheta = \Theta_2(x_s)$ for the desired angle are the solution for such an x_s, and can be treated as the appearance of two contact discontinuities issuing from one point with a wedge stagnant region between them, behind the bifurcation point of the fronts. This question merits more careful discussion.

If three generators of the shock fronts converge at one point, then the general conservation laws connecting the gas parameters in the neighborhood of such a point will generally yield an overdefined system of relationships. To eliminate a possible contradiction, it becomes necessary to increase the arbitrariness in the quantity of initial parameters. The assumption of the presence of a contact discontinuity issuing from the branch point is simplest and sufficient. The next step in increasing the arbitrariness mentioned is assuming the possibility of the appearance of two contact discontinuities, which form two opposite edges of an isobaric

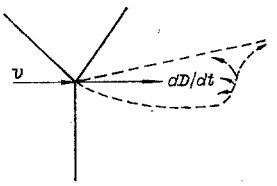

Fig. 13

domain filled with a gas in a relative rest state relative to the branch point of the shocks. Such a domain can be called the wake of the triple point because of the explicit qualitative analogy with an aerodynamic wake behind poorly streamlined bodies.

Under stationary conditions the wake behind a triple point cannot originate, since even tangential stresses of very small magnitude on its boundary cannot at all be equilibrated, and such a formation is severed from a wave configuration in any real stream, rolls up into a vortex, and is entrained by the stream. However, the resultant tangential stress on the wake boundary can be cancelled by the inertial forces during motion of a triple configuration with acceleration directed along the relative freestream velocity vector ahead of the branch point. In this case the vortex-filled wake can exist and be developed because of making up the mass from the exterior stream (Fig. 13), where the solid lines are the shock fronts, the dashes are the contact discontinuities, **v** is the freestream velocity, and D is the rate of displacement of the branch point.

If all the waves have finite intensity, then the velocity head in a stream undergoing two-stage compression is many times greater than the velocity head behind a strong shock. This means that the role of the first of the streams mentioned relative to the second approximates the effect of a solid wall. The boundary with the high-pressure stream becomes almost rectilinear, and liberation of the volume for the developing wake occurs principally because of deformation of the stream passing through an almost normal shock. Therefore, the wake region has the form of a trough behind a cylindrical surface bounding the low-pressure flow domain.

Formation of the trough streamlined by a supersonic stream can be illustrated by the following simple model problem: let the impinging stream be a two-layered flow of an ideal medium separated by a contact discontinuity in the form of a horizontal plane. The velocity above this discontinuity is essentially supersonic, while under the discontinuity the stream is low-pressure, subsonic. The body being streamlined exhibits a dihedral angle with an edge in the plane of the contact discontinuity, perpendicular to the direction of the freestream velocity. The streamlined angle can rotate freely around its edge and has faces of small extent in the flow direction.

The force balance will evidently be such that the upper face of the angle, being subjected to the effect of the high-pressure stream, is practically located in the plane of the contact discontinuity, perturbing the exterior flow slightly. On the other hand, the lower face penetrates deeply into the low-pressure domain, producing a developed separation flow because of deformation of the subsonic stream. A completely analogous effect occurs behind the shock-wave branch point in the situation under consideration. Because of the impossibility of satisfying the conditions of the problem by using the scheme of three shocks with one contact discontinuity, two contact discontinuities with a finite apex angle of the wedge domain between them originate (the analog of the dihedral angle). At least the initial elements of the slip lines behave similarly to the faces of a light wedge, by mainly deforming the stream with relatively low velocity head, i.e., a free volume of the trough type is formed on the surface of the cylinder bounding the subsonic flow.

The flow around such a trough and its development occur under the dominating influence of the exterior supersonic stream.

The shock configuration in a jet becomes unstable upon the impact of the supersonic jet on an obstacle in some sufficiently narrow range of escape parameters, the stationary flow goes spontaneously over into a nonstationary flow, and a self-sustaining strongly fluctuating wave process originates in front of the face side of the obstacle. It is now clear that the internal turbulent wake, which originates and decays periodically behind the bifurcation line of the strong shock fronts, plays the major, probably governing, role in the mechanism of this phenomenon. The application of the results of investigating this phenomenon to analyzing the pulsation modes afforded the possibility of explaining and matching many facts which are experimentally observable.

The stream pulsations are accompanied by significant displacements of the strong central shock along the nonuniform background, whereupon intense entropy waves pass over the subsonic jet behind this shock.

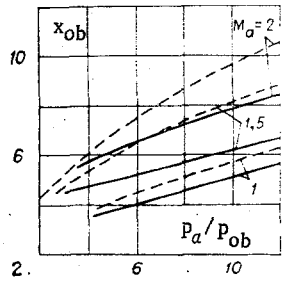

Fig. 14

Several discrete vibrational tones, differing substantially in frequency, are usually observed. The low-frequency pulsations can have a high amplitude and are of fundamental interest for investigations. The amplitude of the high-frequency fluctuations is usually small, and estimates of the frequency show that these fluctuations are associated with processes being propagated with the speed of sound.

An attempt has been made in [2] to construct a simplified mathematical model of this phenomenon on the basis of a one-dimensional description of the nonstationary wave processes under the assumption that the main sampling of the mass in the wake region is concentrated in the tail part of the wake where a sharp change in the stream geometry occurs. This latter circumstance permitted simulation of this phenomenon by a discontinuity in the one-dimensional stream parameters with the inclusion of the area of the active section and the mass discharge. Such a schematization of the flow can be used to describe the initial stage of wake formation, when the dissipative mixing processes exert no essential influence on the dynamics of the phenomenon. At later times, a model with a dominant isobaric mixing of the streams is more preferable.

The difficulty in solving problems as a whole is determined by two main reasons: inadequate study and complexity of the quantitative description of the motion of a triple shock configuration with the formation of a wake behind the bifurcation point and the complex spatial nature of the flow in the neighborhood of the obstacle.

The second reason plays a subordinate role in the problems considered and hence can be satisfied by an approximate approach in the form of the simulating discontinuity considered above, for example.

The wake behind a triple point is that single element of a system which cannot, in principle, exist and be developed under stationary real flow conditions and in this sense is the original cause for the passage to the pulsating interaction mode.

Therefore, there is a foundation to assume that the domain of parameters in which there is no intersection between the curves $\vartheta = \Theta_1(x)$ and $\vartheta = \Theta_2(x)$ (see Fig. 9) is a nonstationary interaction zone. From an analysis of the obtained computational results there follows that the boundary of no stationary solution corresponds (in the terminology of [9]) to the lower boundary of a zone of strong instability. Presented in Fig. 14 is a comparison of these boundaries in the case of jet inflow onto a flat infinite obstacle. The solid line is the boundary of no solution to which $x_{ob} = x^*_{ob}$ corresponds in Fig. 9. Although quantitative agreement is satisfactory just for $M_a = 1$, qualitative agreement holds in all regimes. Similar results have also been obtained for finite obstacles (cylinders with a flat end face).

There is still no satisfactory mathematical model of the fluctuation cycle constructed on the basis of a hypothesis of the periodic origination and decay of the wake behind a triple point.

LITERATURE CITED

1. L. F. Henderson, "On confluence of three shock waves in a perfect gas," Aeronaut. Quart., 15, No. 2 (1964).
2. V. G. Dulov, "On the motion of a triple shock configuration with wake formation behind the branch point," Zh. Prikl. Mekh. Tekh. Fiz., No. 6 (1973).
3. A. G. Golubkov, N. A. Golubkova, and G. I. Smirnova, "Triple shock configurations in hypersonic streams," Izv. Sibirsk. Otd. Akad. Nauk SSSR, Ser. Tekh. Nauk, Ser. 3, No. 1 (1975).
4. V. G. Dulov and G. I. Smirnova, "Analysis of the fundamental free supersonic ideal compressible fluid jet parameters," Zh. Prikl. Mekh. Tekh. Fiz., No. 3 (1971).
5. E. S. Love, C. E. Grigsby, L. P. Lee, and M. J. Woodling, Experimental and Theoretical Studies of Axisymmetric Free Jets, NASA TR-R-6 (1959).
6. A. S. Mikheev, "Analytical solution of the problem of supersonic gas flow around a cone," Vestn. Leningr. Univ., Ser. 7, No. 2 (1962).

7. A. S. Mikheev, "Supersonic gas flow around a body of revolution," Vestn. Leningr. Univ., Ser. 7, No. 2 (1963).
8. A. G. Golubkov and V. G. Dulov, "Supersonic jet interaction with obstacles," Izv. Sibirsk. Otd. Akad. Nauk SSSR, Ser. Tekh. Nauk, Ser. 13, No. 3 (1972).
9. B. G. Semiletenko, B. N. Sobkolov, and V. N. Uskov, "Singularities of the unstable interaction between a supersonic jet and an infinite obstacle," Izv. Sibirsk. Otd. Akad. Nauk SSSR, Ser. Tekh. Nauk, Ser. 13, No. 3 (1972).
10. A. G. Golubkov and V. G. Dulov, "On simulation of the influence of an obstacle placed in a supersonic jet by a conditional discontinuity in the stream parameters," Izv. Sibirsk. Otd. Akad. Nauk SSSR, Ser. Tekh. Nauk, Ser. 3, No. 1, (1975).
11. A. G. Golubkov, B. K. Koz'menko, V. A. Ostapenko, and A. V. Solotchin, "On the interaction between a supersonic underexpanded jet and a plane bounded obstacle," Izv. Sibirsk. Otd. Akad. Nauk SSSR, Ser. Tekh. Nauk, Ser. 13, No. 3 (1972).

ANALYSIS OF THE HYDRODYNAMIC INTERACTION BETWEEN CASCADES OF THIN PROFILES TAKING ACCOUNT OF VORTEX WAKE EVOLUTION

R. L. Kulyaev

UDC 532.582.2

The papers [1-5] are devoted to an investigation of aspects of the hydrodynamic interaction of cascades of profiles in a nonlinear formulation: it is shown experimentally in [1] and theoretically in [2] that the free vortex sheet ruptures upon meeting a profile; taking account of the evolution of vortex wakes, the flows around two cascades of solid profiles of infinitesimal [3] and finite [4] density are computed; results of an experimental investigation of the dynamic reactions of the flow on two mutually moving cascades of thin profiles are presented in [5]. The interference between two cascades of thin profiles in an inviscid, incompressible fluid flow is examined in this paper, where a modified method from [6] is used.

§1. Undetached flow around two cascades of thin profiles by an inviscid incompressible fluid is considered in the plane of the x, y Cartesian coordinates. The y axis is directed along the front of the cascades. The left cascade is assumed fixed, while the right cascade moves along the y axis at the velocity u = const. The flow outside the profiles and their shed vortex wakes are assumed potential, the cascade spacings are identical, the profiles are rigid, and the influence of the wake and profile thicknesses is negligible.

Under the assumptions made, the flow velocity $\mathbf{V} = (V_x, V_y)$ satisfies the equations

$$\operatorname{div} \mathbf{V} = 0, \ \operatorname{rot} \mathbf{V} = 0, \ (x, y) \notin L; \tag{1.1}$$

the periodicity condition

$$\mathbf{V}(x, y + h, t) = \mathbf{V}(x, y, t) \tag{1.2}$$

and the following boundary conditions:

nonpenetration of the fluid through the profile of the cascades

Novosibirsk. Translated from Zhurnal Prikladnoi Mekhaniki i Tekhnicheskoi Fiziki, No. 4, pp. 61-65, July-August, 1976. Original article submitted July 8, 1975.